Revista Brasileira de Ensino de Física, vol. 45, e20230172 (2023)
www.scielo.br/rbef
DOI: https://doi.org/10.1590/1806-9126-RBEF-2023-0172

Classical and quantum systems with position-dependent mass: An application to a Mathews-Lakshmanan-type oscillator

Rieli Tainá Gomes dos Santos[1], Pedro Pablo González-Borrero[*1]

[1]Universidade Estadual do Centro-Oeste, Departamento de Física, Guarapuava, PR, Brasil.

Received on June 27, 2023. Accepted on July 11, 2023.

Position-dependent mass (PDM) systems have diverse applications in physics, attracting significant scientific interest in the last decades. Classical PDM systems pose analytical challenges with their nonlinear equations of motion, while the quantum case is complicated because the kinetic operator is non-Hermitian. To address these challenges, this study explores Hamiltonian factorization and canonical transformations to investigate classical and quantum PDM systems, applying it to a Mathews-Lakshmanan-type oscillator with $m(x) = 1/[1 + (\lambda x)^2]$. Classically, the phase space is examined, revealing increasingly pronounced deformities in the trajectories as energy and λ values increase. In the quantum realm, the solution to the ambiguous ordering problem for the PDM oscillator is presented, accompanied by an analysis of wave functions and probability densities. Further, the tunneling probabilities are analyzed. As λ increases, findings indicate that the tunneling probabilities of the PDM system decrease fast for higher excited states, offering novel insights into its behavior.

Keywords: Position-dependent mass, Mathews-Lakshmanan oscillator, Hamiltonian factorization, point canonical transformations.

1. Introduction

Systems endowed with position-dependent mass have attracted scientists' attention in recent decades due to a wide range of applications in fundamental areas of physics. These systems can be studied from both classical and quantum perspectives. Systems with position-dependent mass are present in the study of electronic and optical properties of semiconductors [1–3], of graded mixed semiconductors [4], and with abrupt heterostructures [5, 6], in quantum dots and wells [2, 7, 8], quantum liquids [9] and within lattices and superlattices [10, 11]. They are also present in the research of the inversion potential for the NH_3 molecule through density functional theory [12], in many-body systems [13], energy spectrum and transition rate for atomic nuclei [14], magnetic monopoles [15], classical and quantum nonlinear oscillators [16–19], and curved spaces [20]. Classically, these systems can be described in the analysis of the hydrodynamic impact of a rigid body against a liquid-free surface [21] and in the dynamics of a falling chain wrapped around a table [22], among others.

Traditionally, the solution methods for a system with position-dependent mass (PDM) are not those usually used for solving a constant mass system. In the case of classical systems with PDM, Newton's Second Law must be extended to allow the analysis of the system's dynamics [23]. However, the equations of motion obtained from the Second Law are nonlinear, making their analytical solution difficult.

Therefore, the unusual methods of Hamiltonian factorization and canonical transformations can facilitate finding the system's solution. Furthermore, the application of canonical transformations aims to relate the system endowed with PDM to a system with constant mass. Besides, Hamiltonian factorization allows the separation of a second-order differential equation into two first-order differential equations [24].

Similarly, a quantum PDM system can be analyzed through uncommon methods since the usual kinetic operator $\hat{T}$ for this system is non-Hermitian. Then, since kinetic energy is required to be a physical observable, the operator representing it must be Hermitian [1]. Thus, to study the dynamics of these quantum systems, the generalized kinetic operator, proposed in Ref. [1], can be used in conjunction with the Hamiltonian factorization method and canonical transformations. With these tools, the dynamics of position-dependent mass systems become workable in the quantum realm.

The harmonic oscillator model is of fundamental importance in physics because many systems with complicated analysis can be reduced or approximated by this model, such as the vibration of atoms in molecules [25]. An example of such model is the nonlinear Mathews-Lakshmanan oscillator [16], which can be treated as a PDM system with $m(x) = 1/[1 + \kappa x^2]$. Mathews-Lakshmanan-type oscillators were previously

[*]Correspondence email address: gonzalez@unicentro.br

studied as PDM systems by different methods in Refs. [19, 24, 26–31].

This paper aims to investigate classical and quantum PDM systems using Hamiltonian factorization and canonical transformations, specifically applied to a Mathews-Lakshmanan-type oscillator. Building upon the work presented in Ref. [24], which employed these methods on an oscillator with the same position-dependent mass, our study seeks to provide a detailed exposition of the Hamiltonian factorization and canonical transformations methods.

In the classical analysis, the phase space for a Matthew-Lakshmanan-type oscillator was previously studied in Ref. [24] for a given energy range. Our study intends to extend those results by presenting the phase space for higher energies and thoroughly interpreting the graphical outcomes.

In the quantum case, Ref. [24] examined the probability density for the state ψ_4 compared to the classical presence. In contrast, this paper analyzes the probability density for lower states considering the potential curve for the system. Furthermore, this study undertook a comprehensive analysis of the tunneling probabilities for a few quantum states of the Mathews-Lakshmanan-type oscillator, introducing a novel perspective on this system's tunneling behavior.

2. Theory of position-dependent mass systems

2.1. Classical case

Consider a classical oscillator-type system with position-dependent mass. The Hamiltonian function for this system is given by

$$H(x,p) = \frac{p^2}{2m(x)} + V(x) \tag{1}$$

where $m(x)$ is a position-dependent function.

The equation of motion for the system is obtained from the Hamiltonian function and is a second-order differential equation, which can be factored into two first-order differential equations. This method is called Hamiltonian factorization and aims to facilitate finding the solution to the system [25].

The factorization is applied using the following ladder functions [32]

$$A^+(x,p) = -i\frac{p}{\sqrt{2m(x)}} + W(x)$$
$$A^-(x,p) = i\frac{p}{\sqrt{2m(x)}} + W(x)$$

where $W(x)$ represents a position-dependent function to be determined.

As in the classical case with constant mass, the ladder functions A^+ and A^- satisfy the commutative property. Then, the factorization method gives rise to a unique Hamiltonian function given by

$$H = A^+A^- = A^-A^+ = \frac{p^2}{2m(x)} + W^2(x) \tag{2}$$

Comparing equations (1) and (2), it is possible to conclude that the potential relates to the function $W(x)$ in a way such that $V(x) = W^2(x)$.

Furthermore, the ladder functions have fundamental relations via Poisson brackets, among them[1] [32]

$$i\{A^-, A^+\} = i\left(\frac{\partial A^-}{\partial x}\frac{\partial A^+}{\partial p} - \frac{\partial A^-}{\partial p}\frac{\partial A^+}{\partial x}\right) = \frac{2W'(x)}{\sqrt{2m(x)}} = 1 \tag{3}$$

$$i\{H, A^+\} = \frac{2W'(x)}{\sqrt{2m(x)}}A^+$$
$$i\{H, A^-\} = \frac{2W'(x)}{\sqrt{2m(x)}}A^-$$

where $W'(x)$ refers to the derivative of $W(x)$ with respect to position x.

From equation (3), one has

$$W'(x) = \sqrt{\frac{m(x)}{2}} \tag{4}$$

The differential equation (4) admits solutions of the form

$$W(x) = \int \sqrt{\frac{m(x)}{2}}dx + C$$

where C refers to the integration constant.

The constant C determines the origin of the potential $V(x)$. Usually, a spatial shift is performed such that $V(x = 0) = 0$ and, consequently, $C = 0$. Therefore, in this case

$$W(x) = \int \sqrt{\frac{m(x)}{2}}dx \tag{5}$$

Since $V(x) = W^2(x)$, then

$$V(x) = \frac{1}{2}\left[\int \sqrt{m(x)}dx\right]^2 \tag{6}$$

and the Hamiltonian of the PDM oscillator can be rewritten in a more general way as

$$H = \frac{p^2}{2m(x)} + \frac{1}{2}\left[\int \sqrt{m(x)}dx\right]^2 \tag{7}$$

Performing strategic canonical transformations on equation (7) allows a connection between the

[1] These fundamental relations are associated with a Heisenberg algebra.

 DOI: https://doi.org/10.1590/1806-9126-RBEF-2023-0172

Hamiltonian function of the system with PDM and that of the harmonic oscillator with constant mass, which has known solutions. Thus, the following point canonical transformations are defined as [32]

$$X(x) = \int \sqrt{m(x)}dx \tag{8}$$

$$P(x,p) = \dot{X}(x) = \frac{p}{\sqrt{m(x)}} \tag{9}$$

Applying the point canonical transformations, equations (8) and (9), into equation (7), it is possible to obtain the general form of the Hamiltonian function for constant mass systems, i.e.,

$$\tilde{H} = \frac{P^2}{2} + \frac{X^2}{2} = E \tag{10}$$

where E represents the energy of the system. Because $\omega = m_0 = 1$ was considered unitary, the trajectories in the phase space are concentric circles and not the usual ellipses.

From equation (10), it is possible to obtain the well-known trajectories $X(t)$ and $P(t)$ for the oscillator with constant mass as

$$X(t) = \sqrt{2E}\cos(t+\phi) \tag{11a}$$

$$P(t) = -\sqrt{2E}\sin(t+\phi) \tag{11b}$$

where ϕ represents the initial phase of the system.

Because the canonical transformations are invertible, it is possible to relate the solutions of the harmonic oscillator with constant mass to the original system with PDM. Then, the trajectories $x(t)$ and $p(t)$ of the system with position-dependent mass are [32]

$$x(t) = X^{-1}[\sqrt{2E}\cos(t+\phi)] \tag{12a}$$

$$p(t) = -\sqrt{m(x(t))}\sin(t+\phi) \tag{12b}$$

with $\sqrt{2E}\cos(t+\phi)$ representing the argument of the inverse function X^{-1}.

Therefore, point canonical transformations applied on a system with position-dependent mass highlight the proximity between the Hamiltonian with PDM and the usual one for a constant mass system. Moreover, this method allows a more straightforward way to find $x(t)$ and $p(t)$ for a PDM system because obtaining them from already-known trajectories is possible.

2.1.1. A classical Mathews-Lakshmanan-type oscillator

Consider a Mathews-Lakshmanan-type oscillator with a mass function $m(x)$ of the form

$$m(x) = \frac{m_0}{1+(\lambda x)^2} \tag{13}$$

where m_0 represents a positive constant value with mass dimension and λ a parameter also positive and constant with the inverse of length dimension.

The mass function $m(x)$ chosen was not completely arbitrary. As already seen, through canonical transformations, equations (8) and (9), it is possible to relate the oscillator with constant mass to the one with PDM. According to Ref. [24], for certain position-dependent mass functions, the canonical transformation referring to $X(x)$ may not map its domain $\mathcal{D}(m(x))$ onto the entire real line. In this case, the mass function is not physically acceptable for relating the oscillators since the position of the particle $X(x)$ does not take real values.

Notice that in the limit where $\lambda \to 0$, one has $m(x) \to m_0$, and there is a tendency to return to a system with constant mass. Moreover, when $x = 0$, the maximum value m_0 is obtained for $m(x)$. On the other hand, when $|x| \to \infty$, then $m(x) \to 0$. Therefore, the function defined by equation (13) is bounded and has a real domain, i.e., it is physically acceptable.

The features above can be observed in Fig. 1(a), in which the mass function $m(x)$ was plotted considering $m_0 = 1$ unitary. From this plot, varying the parameter λ, it is possible to observe that the function $m(x)$ has no singularities. Moreover, when $\lambda \to 0$, the shape of $m(x)$ is smoothed, and $m(x) \to m_0 = 1$, as expected. In addition, for $x = 0$, the curve approaches its maximum value $m(x) = m_0 = 1$, regardless of the λ value. These conclusions obtained by the graphical results corroborate the mathematical interpretations of equation (13).

By inserting the mass function, equation (13), into equation (6) for the potential of the oscillator with position-dependent mass, one obtains

$$V(x) = \frac{m_0}{2\lambda^2}[\sinh^{-1}(\lambda x)]^2 \tag{14}$$

Thus, equation (14) represents the generalized potential energy for the Mathews-Lakshmanan-type oscillator defined in this section. The potential $V(x)$ for the PDM oscillator given by equation (14) was plotted in Fig. 1(b), where $V(x=0) = 0$, respecting the condition initially imposed that $C = 0$ in equation (6).

It can also be noticed from Fig. 1(b) that when $\lambda \to 0$, the curve representing the potential approaches a parabola, similar to the potential curve for the harmonic oscillator with constant mass. In fact, taking the limit of $V(x)$ when $\lambda \to 0$, one has

$$\lim_{\lambda\to 0}\left[\frac{m_0}{2\lambda^2}[\sinh^{-1}(\lambda x)]^2\right] = \frac{x^2}{2} \tag{15}$$

and there is a tendency for the potential $V(x)$ to return to that one associated with the classical harmonic oscillator system, i.e., described by a parabola.

The same result evidenced in equation (15) also occurs for $x \to 0$, i.e., values of x around the origin[2]. Further, Fig. 1(c) indicates that for values of x close to

[2] Another way to notice that is by using Taylor expansion around $x = 0$, that is, considering small oscillations around the origin of the system.

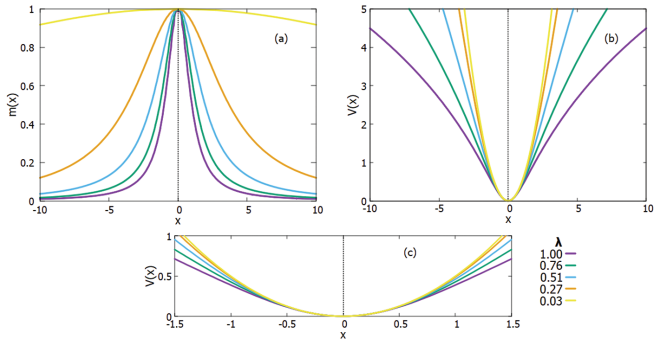

Figure 1: (a) Mass function $m(x)$, with $m_0 = 1$ unitary for different values of λ. (b) Potential $V(x)$ with $m_0 = 1$ unitary for different values of λ. (c) Zoom of the plot (b) for the region around $x = 0$. The parameter was taken as $\lambda = 0.03, 0.27, 0.51, 0.76$, and 1.00 for the three plots.

zero, there is an overlap region for the plots of $V(x)$, regardless of λ values. These curves around $x = 0$ are similar to parabolas. As the horizontal displacement from $x = 0$ occurs and λ increases, the deformations become more evident, and the potential curve departs from the parabolic shape, as observed in Fig. 1(b).

Furthermore, it is important to observe in Fig. 1(b) that when $\lambda = 1$, the system exhibits a larger classically allowed region for movement in comparison to the oscillator with $\lambda = 0.03$. This disparity arises because the potential becomes less confining for higher values of λ.

It is also possible to obtain the trajectories $x(t)$ and $p(t)$ for the oscillator with $m(x)$ through the point canonical transformations represented in equations (8) and (9), with the mass function given by equation (13), in such a way that

$$X(x) = \frac{\sqrt{m_0}}{\lambda}[\sinh^{-1}(\lambda x)] \tag{16a}$$

$$P(x,p) = p\sqrt{\frac{1+(\lambda x)^2}{m_0}} \tag{16b}$$

Then, the trajectory $x(t)$ is obtained using equations (12a) and (12b), such that

$$x(t) = \frac{1}{\lambda}\sinh\left[\sqrt{\frac{2E\lambda^2}{m_0}}\cos(t+\phi)\right] \tag{17}$$

Analogous, the trajectory $p(t)$ is obtained by substituting the mass function (13) and equation (17) into equation (12b). Then,

$$p(t) = -\sqrt{\frac{1}{1+(\lambda x)^2}}\sin(t+\phi)$$

$$p(t) = -\frac{\sqrt{2m_0E}}{\cosh\left[\sqrt{\frac{2E\lambda^2}{m_0}}\cos(t+\phi)\right]}\sin(t+\phi) \tag{18}$$

Considering $m_0 = 1$ unitary and phase shift $\phi = 0$, the trajectories $x(t)$ and $p(t)$ are given by

$$x(t) = \frac{1}{\lambda}\sinh\left[\sqrt{2E\lambda^2}\cos(t)\right] \tag{19}$$

$$p(t) = -\frac{\sqrt{2E}}{\cosh\left[\sqrt{2E\lambda^2}\cos(t)\right]}\sin(t) \tag{20}$$

Furthermore, the Hamiltonian function represented in equation (7) becomes

$$H(x,p) = \frac{[1+(\lambda x)^2]}{2}p^2 + \frac{1}{2\lambda^2}[\sinh^{-1}(\lambda x)]^2 = E \tag{21}$$

The trajectory $x(t)$ represented in equation (19) for the Mathews-Lakshmanan-type oscillator agrees with the trajectory equation obtained in Ref. [19], where the author used the same mass function $m(x)$ as the one in this paper. However, the author obtained the expression for the trajectory $x(t)$ by a different method from the one used in this paper, solving directly the nonlinear differential equation of motion for the system.

The trajectories $x(t)$ and $p(t)$ of the system with position-dependent mass were compared to those for the oscillator with constant mass in Figs. 2(a) and 2(b). In both plots, the parameter λ was considered equal to one for the differences in the behavior of the trajectories of both oscillators be better evidenced.

It can be noticed in Fig. 2(a) that the trajectory $x(t)$ for the system with PDM has a higher amplitude, and the position of the minima and maxima do not vary when compared to the trajectory $X(t)$ for the oscillator with constant mass. In addition, Fig. 2(a) coincides with the trajectories obtained in Fig. 1(b) of Ref. [19], where $x(t)$

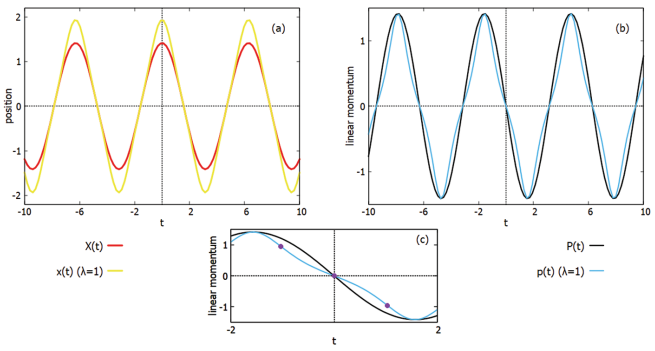

Figure 2: (a) Trajectories $x(t)$, equation (17), in yellow for the oscillator with the mass function $m(x)$ and $X(t)$, equation (11a), in red for the oscillator with constant mass.(b) Trajectories $p(t)$, equation (18), in blue for the oscillator with the mass function $m(x)$ and $P(t)$, equation (11b), in black for the oscillator with constant mass. (c) Zoom of the plot (b) for t values between -2 and 2, showing the inflection points in purple at $t = 1.03$, $t = 0$, and $t = -1.03$.

 DOI: https://doi.org/10.1590/1806-9126-RBEF-2023-0172

was obtained directly by solving the nonlinear equation of motion of the PDM system with the same $m(x)$ used in this paper.

Moreover, the trajectory $p(t)$ for the PDM system is represented in Fig. 2(b). Observe that $p(t)$ has the same amplitude and, also, the same minima and maxima values compared to the trajectory $P(t)$ for the oscillator with constant mass.

Furthermore, the functions sine and cosine in terms of time only have inflection points localized in $t = 0$. In contrast, the hyperbolic cosine has no inflection points in its domain. However, when these trigonometric functions are combined in equation (18), there are more inflection points in the trajectory $p(t)$ besides at $t = 0$ (Fig. 2(c)).

The trajectories in phase space for the PDM oscillator, considering the same energy range as Ref. [24], were obtained using equation (21) and are represented in Fig. 3. From Fig. 3(a), notice that when $\lambda = 0.03$, i.e., $\lambda \to 0$, the trajectories tend to those of the oscillator with constant mass, i.e., concentric circles.

Additionally, Fig. 3(b) shows the trajectories in phase space for $\lambda = 1$ and for the same energy values as in Fig. 3(a). Observe that when $\lambda = 1$, the trajectories' deformations become evident, with the deformity increasing as the energy value E increases. Besides, from Fig. 3(b), it is noticeable that the particle's velocity only cancels out at the return points, regardless of the λ parameter.

Furthermore, from Fig. 3(b), observe that as energy values increase, the curves near the x-axis are more abruptly curved, flattening the trajectory in this direction. As for critical low-energies in Fig. 3(b), for example, $E = 0.05$, even though $\lambda = 1$, the trajectory approaches the one for a constant mass oscillator. In addition, the deformed trajectories in Fig. 3(b) resemble a diamond plot with rounded vertices, being more evidenced for $E \geq 0.30$. Besides, the trajectories in phase space have similar behavior to those obtained in Ref. [24] for the same mass function used in this study.

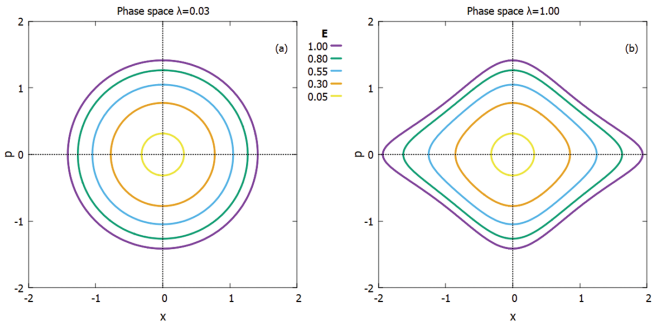

Figure 3: (a) Phase space of the oscillator with function mass $m(x)$ with $m_0 = 1$ and $\lambda = 0.03$ for different energy values. (b) Phase space of the oscillator with PDM with function mass $m(x)$ with $m_0 = 1$ and $\lambda = 1.00$ for different energy values. In both plots, energy values were $E = 0.05, 0.30, 0.55, 0.80$, and 1.00.

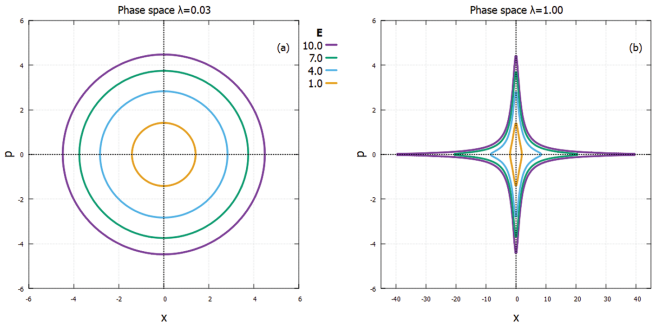

Figure 4: (a) Phase space of the oscillator with function mass $m(x)$ with $m_0 = 1$ and $\lambda = 0.03$ for different energy values. (b) Phase space of the oscillator with PDM with function mass $m(x)$ with $m_0 = 1$ and $\lambda = 1.00$ for different energy values. In both plots, energy values were $E = 1.0, 4.0, 7.0$, and 10.0.

Moreover, Fig. 4 shows the trajectories in phase space considering higher energies than those in Fig. 3. The phase space with $\lambda = 0.03$ is represented in Fig. 4(a). Even though the energy values are higher, the trajectories in this phase space in Fig. 4(a) remain like those for the constant mass oscillator because $\lambda \to 0$. Therefore, the λ parameter has a greater impact on the phase space deformation than the energy values.

In contrast, Fig. 4(b) shows the trajectories in phase space for $\lambda = 1$ for higher energy values than those in Fig. 3. In this case, it is noticeable that the trajectories become highly deformed as E increases. Additionally, one can observe that the x-axis range significantly and rapidly expands as the energy values increase. However, comparing Figs. 4(a) and 4(b), one can note that the maximum values in the p-axis do not vary when λ value change. This result also occurs for lower energies in Fig. 3.

Besides, observe that the scales in Figs. 3(b) and 4(b) are significantly different, then it is not possible to properly interpret the shape of the curves in Fig. 4(b). The trajectories in phase space in Fig. 4(b) have similar behavior to those obtained by a different method than ours in Fig. 1 of Ref. [33]. However, the authors did not specify the energy range used to plot the trajectories, which was done in this paper.

Hence, the differences between the behavior of the Mathews-Lakshmanan-type oscillator and the constant mass oscillator become more evident as energy and λ values increase.

2.2. Quantum case

The Hamiltonian operator for a quantum system endowed with position-dependent mass in the usual form is[3]

$$\hat{H} = \hat{T} + \hat{V} = \frac{\hat{p}^2}{2\hat{m}(\hat{x})} + \hat{V}(\hat{x}) \qquad (22)$$

[3] As the mass is dependent on the position operator $\hat{x}$, the mass in this case also becomes an operator $\hat{m}(\hat{x})$.

Since the mass is a function of the position operator, then $\hat{m}(\hat{x})$ does not commute with $\hat{p}$, and these quantities cannot be simultaneously measured. Therefore, the kinetic energy of this system is not a physical observable.

Thus, the kinetic energy operator $\hat{T}$ represented in equation (22) is non-Hermitian. However, it is desired that the kinetic energy be a measurable quantity. Consequently, the operator $\hat{T}$ representing this quantity must be Hermitian.

In 1983, Roos [1] proposed a generalization of the kinetic energy operator to make the Hamiltonian operator $\hat{H}$ Hermitian. In Roos generalization, the kinetic energy is written as[4] [1]

$$\hat{T} = \frac{1}{4}[m^{\alpha}\hat{p}m^{\beta}\hat{p}m^{\gamma} + m^{\gamma}\hat{p}m^{\beta}\hat{p}m^{\alpha}]$$

Then, the generalized Hamiltonian operator is given by

$$\hat{H} = \frac{1}{4}[m^{\alpha}\hat{p}m^{\beta}\hat{p}m^{\gamma} + m^{\gamma}\hat{p}m^{\beta}\hat{p}m^{\alpha}] + \hat{V}(\hat{x}) \tag{23}$$

with $\hat{p} = -d/dx$ and the parameters α, β and γ satisfying the constraint

$$\alpha + \beta + \gamma = -1 \tag{24}$$

The time-independent Schrödinger equation for quantum systems is

$$\hat{H}\varphi(x) = E\varphi(x) \tag{25}$$

with $\hat{H} = \hat{T} + \hat{V}$.

Then, substituting equation (23) into equation (25), the time-independent Schrödinger equation for the PDM system is generalized as

$$\left(\frac{1}{4}[m^{\alpha}\hat{p}m^{\beta}\hat{p}m^{\gamma} + m^{\gamma}\hat{p}m^{\beta}\hat{p}m^{\alpha}] + V(x) - E\right) \times \varphi(x) = 0$$

Therefore, the kinetic energy operator becomes Hermitian when the parameters obey the constraint in equation (24). However, the choice of the parameters α, β, and γ is not unique [34, 35], i.e., different values of parameters generate distinct and non-equivalent Hamiltonian operators to give rise to an ambiguous ordering problem [36].

Literature contains several studies advocating the choice of a specific set of parameters [4, 37–40]. Even before the generalization of the Hamiltonian operator $\hat{H}$ performed by Roos, papers were published proposing a new form for the kinetic energy operator $\hat{T}$ to study systems with position-dependent mass [4, 37].

[4] In this section, the mass operator $\hat{m}(\hat{x})$ will be represented simply as m or $m(x)$ to simplify the notation. However, the mass remains an operator with spatial dependence on $\hat{x}$.

After the Roos generalization, researchers found that the previously proposed Hamiltonian operators represent a specific case of the generalized operator with a given set of parameters α, β, and γ. In addition, other sets of parameters were studied after the generalization that had not been previously analyzed [38, 40].

In 1966, BenDaniel and Duke [37] proposed a modified Hamiltonian to study systems with position-dependent mass. The Hermitian operator suggested by these authors is recovered in the Roos generalization by considering $\alpha = \gamma = 0$ and $\beta = -1$. In 1969, Gora and Williams [4] proposed a Hamiltonian operator such that, in the Roos generalization, $\alpha = -1$ and $\beta = \gamma = 0$ to study semiconductors with smoothly graded composition, i.e., a system in which the effective mass is position-dependent.

In 1983, Zhu and Kroemer [39] proposed a Hermitian Hamiltonian where $\alpha = \gamma = -1/2$ and $\beta = 0$ to study the wave functions with position-dependent effective mass in an abrupt heterojunction between two semiconductors. Furthermore, in 1993, Li and Kuhn [38] analyzed the case where $\alpha = 0$ and $\beta = \gamma = -1/2$ to study a heterojunction in which the mass function varies smoothly with the position. Finally, in 2007, Mustafa and Mazharimousavi [40] proposed a Hermitian Hamiltonian operator with the parameters $\alpha = \gamma = -1/4$ and $\beta = -1/2$ in the generalization performed by Roos.

There is an interesting discussion in the article written by Morrow and Brownstein [6] in 1984, in which the authors showed that $\alpha = \gamma$. This equality is because of the condition of continuity of $\psi'(x,t)/m(x)$ in abrupt heterojunctions between two crystals, i.e., when there is a non-finite discontinuity in the effective mass of the system [41]. Therefore, in this case, the Hamiltonian operator becomes [6]

$$\hat{H} = \frac{1}{2}\,[m^{\alpha}\ \hat{p}\ m^{\beta}\ \hat{p}\ m^{\alpha}] + \hat{V}(\hat{x}) \tag{26}$$

with the constraint

$$2\alpha + \beta = -1$$

In this study, although the analyzed system is not a semiconductor with abrupt heterojunction, $\alpha = \gamma$ will be used due to the physical viability of the condition.

To apply the Hamiltonian factorization method, the operator represented in equation (26) will be used, considering $\alpha = a$, $\beta = 2b$, and $\hat{p} = -d/dx$ to simplify the notation. Then

$$\hat{H} = -\frac{1}{2}m^{a}\frac{d}{dx}m^{2b}\frac{d}{dx}m^{a} + \hat{V}(\hat{x}) \tag{27}$$

with the constraint

$$a + b = -1/2 \tag{28}$$

 DOI: https://doi.org/10.1590/1806-9126-RBEF-2023-0172

In addition, the following ladder operators are defined [42]

$$\hat{A}_a^- = \frac{1}{\sqrt{2}} m^b \frac{d}{dx} m^a + W_a(\hat{x}) \tag{29}$$

$$\hat{A}_a^+ = -\frac{1}{\sqrt{2}} m^a \frac{d}{dx} m^b + W_a(\hat{x}) \tag{30}$$

where $W_a(\hat{x})$ is called "superpotential".

Moreover, as the quantum harmonic oscillator with constant mass, the operators $\hat{A}_a^+$ and $\hat{A}_a^-$ obey the following commutation relation [42]

$$[\hat{A}_a^-, \hat{A}_a^+] = 1 \tag{31}$$

Equation (31) shows that the ladder operators $\hat{A}_a^+$ and $\hat{A}_a^-$ do not commute. This gives rise to two Hamiltonian operators, $\hat{H}_a^-$ and $\hat{H}_a^+$, such that [42]

$$\begin{aligned} \hat{H}_a^+ &= \hat{T}_a^+ - \left(\frac{W_a}{\sqrt{2m}}\right)' - 4aW_a \left(\frac{1}{\sqrt{2m}}\right)' + W_a^2 \\ &= \hat{T}_a^+ + \hat{V}_a^+ \end{aligned} \tag{32}$$

and

$$\begin{aligned} \hat{H}_a^- &= \hat{T}_a^- - \left(\frac{W_a}{\sqrt{2m}}\right)' - 4aW_a \left(\frac{1}{\sqrt{2m}}\right)' + \frac{2W_a'}{\sqrt{2m}} + W_a^2 \\ &= \hat{T}_a^- + \hat{V}_a^- \end{aligned} \tag{33}$$

where the kinetic energy operators $\hat{T}_a^+$ and $\hat{T}_a^-$ are given by

$$\hat{T}_a^+ = -\frac{1}{2} m^a \frac{d}{dx} m^{2b} \frac{d}{dx} m^a$$

$$\hat{T}_a^- = -\frac{1}{2} m^b \frac{d}{dx} m^{2a} \frac{d}{dx} m^b$$

and the potentials are

$$\hat{V}_a^+ = -\left(\frac{W_a}{\sqrt{2m}}\right)' - 4aW_a \left(\frac{1}{\sqrt{2m}}\right)' + W_a^2 \tag{34}$$

$$\hat{V}_a^- = -\left(\frac{W_a}{\sqrt{2m}}\right)' - 4aW_a \left(\frac{1}{\sqrt{2m}}\right)' + \frac{2W_a'}{\sqrt{2m}} + W_a^2 \tag{35}$$

The potential $\hat{V}_a^-$ represented by equation (35) differs from that obtained in Ref. [24], where their potential has an extra term[5]. However, the potential $\hat{V}_a^-$ equation (35) agrees with the one obtained in Ref. [42]. The derivation of the potential $\hat{V}_a^-$ in equation (35) is presented in the Appendix of the Supplementary Material.

Expanding the commutation relation represented in equation (31), one has

$$\begin{aligned} [\hat{A}_a^-, \hat{A}_a^+] = 1 &\iff \hat{A}_a^- \hat{A}_a^+ - \hat{A}_a^+ \hat{A}_a^- = 1 \\ &\iff \hat{A}_a^- \hat{A}_a^+ - \frac{1}{2} = \hat{A}_a^+ \hat{A}_a^- + \frac{1}{2} \end{aligned} \tag{36}$$

with the Hamiltonian operator $\hat{H}$ characteristic of a harmonic oscillator

$$\begin{aligned} \hat{H} = \hat{A}_a^- \hat{A}_a^+ - \frac{1}{2} = \hat{A}_a^+ \hat{A}_a^- + \frac{1}{2} \\ \implies \hat{H} = \hat{H}_a^- - \frac{1}{2} = \hat{H}_a^+ + \frac{1}{2} \end{aligned} \tag{37}$$

According to equation (37), the supersymmetric partners $\hat{H}_a^-$ and $\hat{H}_a^+$ have the same spectrum, however, $\hat{H}_a^-$ has one less bound state than its partner $\hat{H}_a^+$ [43].

Substituting the equations (32) and (33) into the commutator relation, equation (36), one has that

$$\hat{T}_a^- + \frac{2W_a'}{\sqrt{2m}} - 1 = \hat{T}_a^+ \tag{38}$$

In addition, equation (37) suggests that $\hat{H}$ must be unique. Therefore, the following condition [42]

$$\frac{2W_a'}{\sqrt{2m}} - 1 = 0 \implies W_a' = \frac{\sqrt{2m}}{2} \tag{39}$$

is imposed in equation (38).

The solution of the differential equation represented in equation (39) is given by

$$W_a = \frac{1}{\sqrt{2}} \int \sqrt{m(x)}\, dx \tag{40}$$

Since the potential terms in equation (38) were canceled out, then $\hat{T}_a^+ = \hat{T}_a^-$, i.e.,

$$-\frac{1}{2} m^a \frac{d}{dx} m^{2b} \frac{d}{dx} m^a = -\frac{1}{2} m^b \frac{d}{dx} m^{2a} \frac{d}{dx} m^b \tag{41}$$

and for equation (41) to be satisfied, it is necessary that $a = b$.

In addition, using the constraint equation (28), it is possible to infer that $a = b = -1/4$. In this case, since $\alpha = \gamma = a$ and $\beta = 2b$, one has

$$\alpha = \gamma = -\frac{1}{4}; \qquad \beta = -\frac{1}{2} \tag{42}$$

and the ambiguous ordering problem is solved for the harmonic oscillator, as done in Ref. [42]

Thus, with $a = -1/4$ and equation (34), the potential $\hat{V}_{-1/4}^+$ become

$$\hat{V}_{-1/4}^+ = -\frac{W_{-1/4}'}{\sqrt{2m}} + W_{-1/4}^2 = W_{-1/4}^2 - \frac{1}{2} \tag{43}$$

$$\hat{V}_{-1/4}^- = \frac{W_{-1/4}'}{\sqrt{2m}} + W_{-1/4}^2 = W_{-1/4}^2 + \frac{1}{2} \tag{44}$$

using equation (39) for both cases to infer that

$$\frac{W_{-1/4}'}{\sqrt{2m}} = \frac{1}{2}$$

As evidenced by equations (43) and (44), the potentials $\hat{V}_{-1/4}^+$ and $\hat{V}_{-1/4}^-$ are supersymmetric partners, as proved in Ref. [42].

[5] The potential used by the authors results in an approximation for solving the ambiguous ordering problem.

Furthermore, it is possible to notice that the superpotential represented in equation (40) has the same form as the function $W(x)$ in equation (5), obtained by factoring the Hamiltonian of the classical oscillator with position-dependent mass.

To analyze the existing relationship between the superpotential $W_{-1/4}(\hat{x})$ and the potential $\hat{V}(\hat{x})$, equation (37) and the previously obtained parameter $a = -1/4$ are used. Thus

$$\begin{aligned}
&\hat{H} = \hat{H}^{+}_{-1/4} + \frac{1}{2} \\
&\hat{T}^{+}_{-1/4} + \hat{V}(\hat{x}) = \hat{T}^{+}_{-1/4} + \hat{V}^{+}_{-1/4}(\hat{x}) + \frac{1}{2} \\
&V(\hat{x}) = W^2_{-1/4} - \frac{1}{2} + \frac{1}{2} \\
&V(\hat{x}) = W^2_{-1/4}
\end{aligned}$$

with $\hat{H}$ given by equation (27) and $\hat{H}^{+}_{-1/4}$ given by equation (32).

Therefore, the potential $V(x)$ for the quantum oscillator with PDM is given by

$$\hat{V}(x) = \frac{1}{2}\left[\int \sqrt{m(x)}\, dx\right]^2 \tag{45}$$

which has the same form of the potential given by equation (6) obtained for the classical case of a PDM oscillator. Hence, with the parameter set of Mustafa and Mazharimousavi [40] (equation (42)), a correspondence between the classical and quantum position-dependent mass oscillators could be established [42].

Furthermore, the Hamiltonian operator with the parameter set of Mustafa and Mazharimousavi is given by

$$\hat{H} = \frac{1}{2}\,\frac{1}{\sqrt[4]{m}}\,\hat{p}\,\frac{1}{\sqrt{m}}\,\hat{p}\,\frac{1}{\sqrt[4]{m}} + \hat{V}(\hat{x}) \tag{46}$$

Then, using equation (46) and equation (45), one has

$$\hat{H} = \frac{1}{2}\frac{1}{\sqrt[4]{m}}\hat{p}\frac{1}{\sqrt{m}}\hat{p}\frac{1}{\sqrt[4]{m}} + \frac{1}{2}\left[\int \sqrt{m}\, dx\right]^2 \tag{47}$$

The kinetic energy operator for the quantum harmonic oscillator with position-dependent mass represented in the first term of equation (47) is now unique since the Roos parameters were established for this system [42].

Moreover, with $a = b = -1/4$, the ladder operators, equations (29) and (30), become

$$\begin{aligned}
\hat{A}^{-}_{-1/4} &= \frac{1}{\sqrt{2}}\left[\frac{1}{\sqrt[4]{m}}\frac{d}{dx}\frac{1}{\sqrt[4]{m}} + \int \sqrt{m}\, dx\right] \\
\hat{A}^{+}_{-1/4} &= -\frac{1}{\sqrt{2}}\left[\frac{1}{\sqrt[4]{m}}\frac{d}{dx}\frac{1}{\sqrt[4]{m}} + \int \sqrt{m}\, dx\right]
\end{aligned}$$

and when $m(x) \to m_0$, the ladder operators return to those usually used in solving the quantum harmonic oscillator with constant mass.

Therefore, the Hamiltonian factorization method for systems with position-dependent mass allows the finding of the appropriate ladder operators to analyze the dynamics of systems with PDM. Thus, this method becomes a powerful mathematical tool to simplify solving these systems.

Due to the properties of the ladder operators $\hat{A}^{+}$ and $\hat{A}^{-}$, the same relations for the case of the quantum harmonic oscillator with constant mass are obtained, that is

$$\begin{aligned}
&\hat{A}^{-}_{-1/4}\psi_0(x) = 0 \\
&\hat{A}^{-}_{-1/4}\psi_n(x) = \sqrt{n}\psi_{n-1}(x) \\
&\hat{A}^{+}_{-1/4}\psi_n(x) = \sqrt{n+1}\psi_{n+1}(x)
\end{aligned}$$

with the wave function given by

$$\psi_n(x) = \frac{1}{\sqrt{n!}}(\hat{A}^{+}_{-1/4})^n\psi_0(x)$$

In addition, it is possible to relate the Hamiltonian operator with position-dependent mass represented in equation (47) to the operator $\hat{H}_0$[6] that describes the oscillator with constant mass.

Initially, consider the eigenvalue equation for the Hamiltonian operator $\hat{H}_{-1/4}$, given by

$$\left[\frac{1}{2}\frac{1}{\sqrt[4]{m}}\hat{p}\frac{1}{\sqrt{m}}\hat{p}\frac{1}{\sqrt[4]{m}} + \frac{1}{2}\left(\int \sqrt{m}\, dx\right)^2\right]\psi_n = E_n\psi_n \tag{48}$$

with $E_n = (n + 1/2)$, in which was taken $\hbar = \omega = 1$. Notice that because of the form of E_n, it is possible to infer that the PDM oscillator is in the same class as the harmonic oscillator with constant mass because they have the same energy spectrum, although having different potentials [44].

Now, using the following canonical point transformations [45]

$$X(x) = \int \sqrt{m}dx \tag{49}$$

$$\psi_n(x) = \sqrt[4]{m}\varphi_n(X) \tag{50}$$

in the eigenvalue equation (48), and considering

$$\begin{aligned}
&\frac{d\varphi_n}{dx} = \frac{d\varphi_n}{dX}\frac{dX}{dx} = \sqrt{m}\,\frac{d\varphi_n}{dX} \\
&\frac{d}{dx}\left(\frac{d\varphi_n}{dX}\right) = \sqrt{m}\,\frac{d^2\varphi_n}{dX^2}
\end{aligned}$$

equation (48) becomes

$$-\frac{1}{2}\frac{d^2\varphi_n}{dX^2} + \frac{1}{2}X^2\varphi_n = E_n\varphi_n \tag{51}$$

[6] The Hamiltonian operator for a system with constant mass is $\hat{H}_0 = \frac{\hat{p}^2}{2m_0} + \hat{V}(\hat{x})$, where m_0 represents the constant mass and $\hat{V}(\hat{x})$ the potential operator.

 DOI: https://doi.org/10.1590/1806-9126-RBEF-2023-0172

Equation (51) is similar to the eigenvalue equation for the quantum harmonic oscillator with constant mass. In fact, the wave functions $\varphi_n(x)$ for equation (51) is the same as that of the harmonic oscillator with constant mass [46], i.e.

$$\varphi_n(X) = \frac{1}{\sqrt{\sqrt{\pi}2^n n!}} \exp\left(-\frac{X^2}{2}\right) \mathcal{H}_n(X)$$

where $\mathcal{H}_n(x)$ represents the Hermite polynomials.

Returning to the solution for the position-dependent harmonic oscillator using the inverse canonical transformation of equations (49) and (50), one has that

$$\begin{aligned}\psi_n(x) = & \frac{1}{\sqrt{\sqrt{\pi}2^n n!}} \sqrt[4]{m(x)} \\ & \times \exp\left(-\frac{(\int \sqrt{m(x)}dx)^2}{2}\right) \\ & \times \mathcal{H}_n\left(\int \sqrt{m(x)}dx\right)\end{aligned} \tag{52}$$

Therefore, equation (52) represents the eigenfunctions of the quantum harmonic oscillator with position-dependent mass. Notice that the Hermite polynomial now has a position dependence as well.

2.2.1. A quantum Mathews-Lakshmanan-type oscillator

As an application to the theory developed in the previous section, consider a Mathews-Lakshmanan-type oscillator with a mass operator defined as

$$\hat{m}(x) = \frac{m_0}{1 + (\lambda\hat{x})^2} \tag{53}$$

with $m_0 = 1$ unitary.

Firstly, it is noticeable from equation (45) that the potential energy for this system will have the same shape as the potential of the classical Mathews-Lakshmanan-type oscillator, represented in equation (14), showing a similarity between both systems.

Besides, from the canonical transformation in equation (49), one has

$$X(x) = \frac{1}{\lambda}\sinh^{-1}(\lambda x)$$

and, thus, it is possible to obtain the eigenfunctions from equation (52), given by

$$\begin{aligned}\psi_n(x) = & \frac{1}{\sqrt{\sqrt{\pi}2^n n!}} \sqrt[4]{\frac{1}{1 + (\lambda x)^2}} \\ & \times \exp\left(-\frac{(\sinh^{-1}(\lambda x))^2}{2\lambda^2}\right) \\ & \times \mathcal{H}_n\left(\frac{\sinh^{-1}(\lambda x)}{\lambda}\right)\end{aligned} \tag{54}$$

In addition, the Hamiltonian operator for the oscillator with function mass defined in equation (53) is given by

$$\begin{aligned}\hat{H} = & -\frac{1}{2}\sqrt[4]{1 + (\lambda x)^2}\frac{d}{dx}\sqrt{1 + (\lambda x)^2} \\ & \times \frac{d}{dx}\sqrt[4]{1 + (\lambda x)^2} + \left[\frac{1}{2\lambda^2}(\sinh^{-1}(\lambda x))^2\right]\end{aligned}$$

From equation (54), the first three eigenfunctions for our Mathews-Lakshmanan-type oscillator are

$$\begin{aligned}\psi_0(x) = & \frac{1}{\sqrt{\sqrt{\pi}}} \sqrt[4]{\frac{1}{1 + (\lambda x)^2}} \\ & \times \exp\left(-\frac{(\sinh^{-1}(\lambda x))^2}{2\lambda^2}\right)\end{aligned} \tag{55}$$

$$\begin{aligned}\psi_1(x) = & \frac{1}{\sqrt{2\sqrt{\pi}}} \sqrt[4]{\frac{1}{1 + (\lambda x)^2}} \\ & \times \exp\left(-\frac{(\sinh^{-1}(\lambda x))^2}{2\lambda^2}\right) \\ & \times \left(\frac{2\sinh^{-1}(\lambda x)}{\lambda}\right)\end{aligned} \tag{56}$$

$$\begin{aligned}\psi_2(x) = & \frac{1}{\sqrt{2\sqrt{\pi}}} \sqrt[4]{\frac{1}{1 + (\lambda x)^2}} \\ & \times \exp\left(-\frac{(\sinh^{-1}(\lambda x))^2}{2\lambda^2}\right) \\ & \times \left[\left(\frac{2(\sinh^{-1}(\lambda x))^2}{\lambda^2}\right) - 1\right]\end{aligned} \tag{57}$$

$$\begin{aligned}\psi_3(x) = & \frac{1}{\sqrt{3\sqrt{\pi}}} \sqrt[4]{\frac{1}{1 + (\lambda x)^2}} \\ & \times \exp\left(-\frac{(\sinh^{-1}(\lambda x))^2}{2\lambda^2}\right) \\ & \times \left[2\left(\frac{\sinh\lambda x}{\lambda}\right)^3 - 3\left(\frac{\sinh^{-1}(\lambda x)}{\lambda}\right)\right]\end{aligned} \tag{58}$$

With equations (55)–(58), it is possible to plot the wave functions and probability distributions for the Mathews-Lakshmanan-type oscillator, represented in Figs. 5 and 6, respectively.

The plots for the wave functions for the PDM system with $m(x)$ represented in Fig. 5 agree with the ones obtained for the same quantum system in Ref. [24]. However, in our study, the wave functions for the PDM system were plotted with those for the constant mass oscillator to enable a further investigation of the similarities and differences between both oscillators.

From Fig. 5, it is noticeable that the wave functions for the oscillator with position-dependent mass preserve symmetry about the y-axis. Analogous to the case of the quantum harmonic oscillator with constant mass, this symmetry is due to the Hermite polynomials $\mathcal{H}_n(x)$

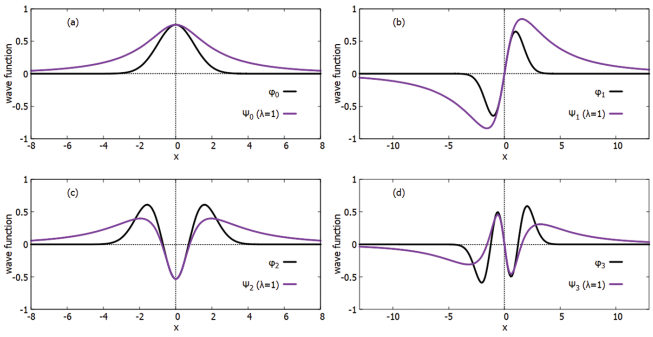

Figure 5: Wave functions (a) $\psi_0(x)$ and $\varphi_0(x)$, (b) $\psi_1(x)$ and $\varphi_1(x)$, (c) $\psi_2(x)$ and $\varphi_2(x)$, (d) $\psi_3(x)$ and $\varphi_3(x)$ with $m_0 = \lambda = 1$. The wave functions $\psi_n(x)$ describe the harmonic oscillator with $m(x)$ (in purple), and $\varphi_n(x)$ describe the harmonic oscillator with constant mass (in black).

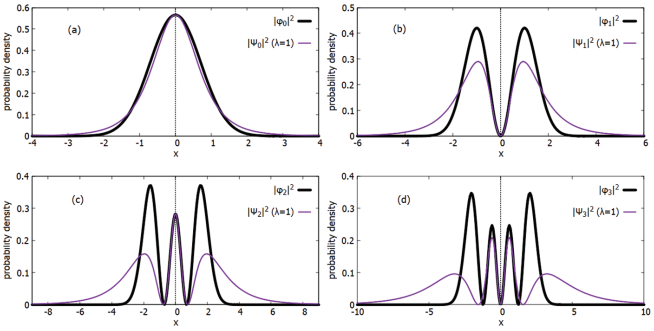

Figure 6: Probability densities (a) $|\psi_0(x)|^2$ and $|\varphi_0(x)|^2$, (b) $|\psi_1(x)|^2$ and $|\varphi_1(x)|^2$, (c) $|\psi_2(x)|^2$ and $|\varphi_2(x)|^2$, (d) $|\psi_3(x)|^2$ and $|\varphi_3(x)|^2$ with $m_0 = \lambda = 1$. The probability densities $|\psi_n(x)|^2$ are related to the harmonic oscillator with $m(x)$ (in purple) and $|\varphi_n(x)|^2$ with the harmonic oscillator with constant mass (in black).

having definite parity, with $\mathcal{H}_{2n}$ even and $\mathcal{H}_{2n+1}$ odd. Therefore, the wave functions ψ_{2n} remain to have even parity, and ψ_{2n+1} preserves its odd parity.

From equation (54), one can observe that when $\lambda \to 0$, the wave functions tend to those for the oscillator with constant mass. This result also occurs for x values close to zero. Notice in Fig. 5 that around $x = 0$ values, there is an overlap region of the curves representing the oscillator with constant mass and the one with PDM. The superposition regions indicate that both oscillators have similar behavior around the origin, even though $\lambda = 1$.

The probability densities for the constant mass and the PDM oscillators were plotted in Fig. 6. It is noticeable that for the Mathews-Lakshmanan-type oscillator, the distribution seems to be more spread out in contrast to the probability density for the oscillator with constant mass. Then, from Fig. 6, one could infer that the PDM system is more spatially dispersed, i.e., has a less defined position. However, it is crucial to consider that the PDM system has a different potential shape than that of the constant mass oscillator.

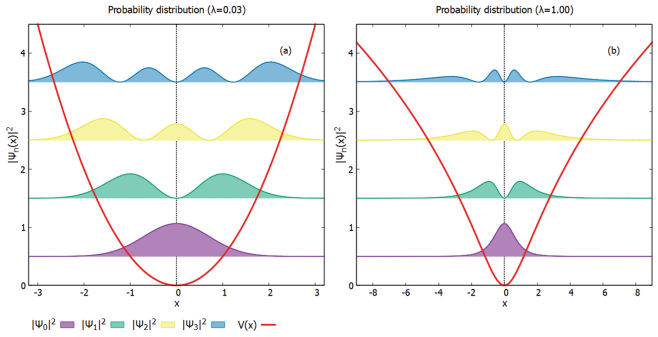

Figure 7: Potential (equation (45)) and probability densities of $|\psi_0(x)|^2$ (lower level), $|\psi_1(x)|^2$, $|\psi_2(x)|^2$, and $|\psi_3(x)|^2$ (higher level) for (a) $\lambda = 0.03$ and (b) $\lambda = 1$. The probability densities $|\psi_n(x)|^2$ were dislocated regarding the y-axis in a factor of $1/2$, the incremental of each energy level.

The probability densities were plotted with the potential curve in Fig. 7. The potential for the system with $\lambda = 1$ represented in Fig. 7(a) is less confining compared to the oscillator with $\lambda = 0.03$ in Fig. 1(b), which resemble a parabola. Then, this indicates that the oscillator with $\lambda = 1$ has a larger classically allowed region of movement, as seen in Fig. 7(b) (notice the difference between the x-axis ranges in Figs. 7(a) and 7(b)).

Additionally, Fig. 7(a) shows that when $\lambda = 0.03$, i.e., $\lambda \to 0$, the potential and probability densities approach those for the oscillator with constant mass. In this case, the particle has higher probability densities at the extremities of the classically allowed region delimited by the potential, as expected.

Contrary to what Fig. 6 might indicate, Fig. 7(b) suggests that the particle is more likely to be detected around the system's origin and not at the extremities of the classically allowed region. This conclusion is not trivial to be inferred only by analyzing Fig. 6 because the probability densities are not shown with the potential curve in Fig. 1(b).

Further, as well-known, there is a close relation between the probability density of the system and the tunneling probability through the potential barrier. For the oscillator with $\lambda \to 0$, Fig. 7(a) indicates that the tunneling probability decreases slowly for higher excited states, as for the oscillator with constant mass.

In contrast, for the system with $\lambda = 1$, Fig. 7(b) shows that for the state corresponding to $n = 0$, the system has an equally high probability of tunneling compared to the same state in Fig. 7(a). This closeness of tunneling probabilities comes from the similarity between the probability density curves in Fig. 6(a). However, one can observe in Fig. 7(b) that for the quantum state $n = 1$, the tunneling probability decreases significantly in contrast with the same quantum state in Fig. 7(a).

Yet, the tunneling probability decays more noticeably and even faster for higher excited states ($n = 2$ and 3). For instance, notice the difference in the quantum state corresponding to $n = 3$ between the Figs. 7(a) and 7(b).

 DOI: https://doi.org/10.1590/1806-9126-RBEF-2023-0172

Therefore, the PDM system with a lower λ value is more likely to tunnel through the potential barrier in this quantum state.

3. Conclusions

This study enhanced the comprehension of classical and quantum systems with position-dependent mass. The analytical challenges of nonlinear equations of motion and non-Hermitian operators were addressed through Hamiltonian factorization and canonical transformations methods for both systems. The theory was applied on a Mathews-Lakshmanan-type oscillator with $m(x) = 1/[1 + (\lambda x)^2]$.

Classically, the trajectories in phase space for a Mathews-Lakshmanan-type oscillator were investigated. As the energy and λ values increased, more evident were the trajectories' deformities, and higher was the tendency of those to flatter in the x-direction. This analysis provided an understanding of the system's dynamics and highlighted the significant impact of the λ value in this PDM oscillator.

In the quantum realm, the generalized kinetic energy operator proposed by Von Roos was employed to address the kinetic operator being non-Hermitian, and the solution to the ambiguous ordering problem for the PDM oscillator was presented. Moreover, the wave functions and probability densities were analyzed for a few states of the Mathews-Lakshmanan-type oscillator. Further, this study also investigated the tunneling probabilities for this PDM oscillator. As the λ value increased, the tunneling probability decreased, being more evident for higher excited states. This result offers novel insights into the behavior of the Mathews-Lakshmanan-type oscillator.

Thus, this study contributed to the broader understanding of PDM systems and their dynamics, with implications for various fields of physics where position-dependent mass plays a crucial role.

Acknowledgments

The authors would like to thank the Writing Center (CERTA – Centro de Escrita, Revisão e Tradução Acadêmica – http://www3.unicentro.br/centrodeescritaacademica – of the Midwestern State University of Paraná (UNICENTRO) for assistance with English language developmental editing.

Supplementary material

The following online material is available for this article: Appendix – The potential V_a^-

References

[1] O. von Roos, Phys. Rev. B **27**, 7547 (1983).
[2] R.A. El-Nabulsi, J. of Physics and Chemistry of Solids **140**, 109384 (2020).
[3] G. Bastard, *Wave mechanics applied to semiconductor heterostructures* (Les Editions de Physique, Les Ulis, 1988).
[4] T. Gora and F. Williams, Phys. Rev. **177**, 1179 (1969).
[5] G.T. Einevoll and P.C. Hemmer, J. of Phys. C: Solid State Phys. **21**, L1193 (1988).
[6] R.A. Morrow and K.R. Brownstein, Phys. Rev. B **30**, 678 (1984).
[7] P. Harrison and A. Valavanis, *Quantum wells, wires and dots: theoretical and computational physics of semiconductor nanostructures* (John Wiley & Sons, Hoboken, 2016).
[8] R. Khordad, Physica B: Condensed Matter **406**, 3911 (2011).
[9] F.A. Saavedra, J. Boronat, A. Polls and A. Fabrocini, Phys. Rev. B **50**, 4248 (1994).
[10] G. Bastard, Phys. Rev. B **24**, 5693 (1981).
[11] R.A. El-Nabulsi, Physica E: Low-dimensional Systems and Nanostructures **127**, 114525 (2021).
[12] N. Aquino, G. Campoy and H. Yee-Madeira, Chemical Phys. Lett. **296**, 111 (1998).
[13] K. Bencheikh, K. Berkane and S. Bouizane, J. of Phys. A: Mathematical and General **37**, 10719 (2004).
[14] M. Alimohammadi, H. Hassanabadi and S. Zare, Nuclear Physics A **960**, 78 (2017).
[15] A.L. Jesus and A.G.M. Schmidt, J. of Mathematical Physics **60**, 122102 (2019).
[16] P.M. Mathews and M. Lakshmanan, Quarterly of Applied Mathematics **32**, 215 (1974).
[17] J.F. Cariñena, A.M. Perelomov, M.F. Ranada and M. Santander, J. of Phys. A: Mathematical and Theoretical **41**, 085301 (2008).
[18] Á. Ballesteros, A. Enciso, F.J. Herranz, O. Ragnisco and D. Riglioni, International J. of Theoretical Physics **50**, 2268 (2011).
[19] O. Mustafa, The Euro. Phys. Journal Plus **136**, 249 (2021).
[20] C. Quesne and V.M. Tkachuk, J. of Phys. A: Mathematical and General **37**, 4267 (2004).
[21] C.P. Pesce, J. of Applied Mechanics **70**, 751 (2003).
[22] A. Cayley, Proceedings of the Royal Society of London **8**, 506 (1856).
[23] W.C. Guttner and C.P. Pesce, J. of the Brazilian Society of Mechanical Sciences and Engineering **39**, 1969 (2017).
[24] S. Cruz y Cruz, J. Negro and L. Nieto, Phys. Lett. A **369**, 400 (2007).
[25] S.H. Dong, *Factorization Method in Quantum Mechanics* (Springer, Berlin, 2007).
[26] J.F. Cariñena, M.F. Rañada and M. Santander, Reports on Mathematical Physics **54**, 285 (2004).
[27] J.F. Cariñena, M.F. Rañada and M. Santander, Ann. of Phys. **322**, 434 (2007).
[28] S. Cruz y Cruz, Symmetry, Integrability and Geometry: Methods and Applications SIGMA **9**, 4 (2013).

[29] B. Bagchi, S. Das, S. Ghosh and S. Poria, J. of Phys. A: Mathematical and Theoretical **46**, 032001 (2012).
[30] B.G. Costa, I.S. Gomez and M. Portesi, J. of Mathematical Physics **61**, 082105 (2020).
[31] O. Mustafa, Physica Scripta **96**, 065205 (2021).
[32] S. Cruz y Cruz, J. Negro and L.M. Nieto, J. of Phys.: Conference Series **128**, 012053 (2008).
[33] M. Lakshmanan and V.K. Chandrasekar, Eur. Phys. J. Spec. Top. **222**, 665 (2013).
[34] O. Mustafa and S.H. Mazharimousavi, J. of Phys. A: Mathematical and General **39**, 10537 (2006).
[35] J.M. Lévy-Leblond, Phys. Rev. A **52**, 1845 (1995).
[36] T. Bibi, S. Javed and S. Iqbal, Communications in Theoretical Phys. **75**, 015102 (2023).
[37] D.J. BenDaniel and C.B. Duke, Phys. Rev. **152**, 683 (1966).
[38] T.L. Li and K.J. Kuhn, Phys. Rev. B **47**, 12760 (1993).
[39] Q.G. Zhu and H. Kroemer, Phys. Rev. B **27**, 3519 (1983).
[40] O. Mustafa and S.H. Mazharimousavi, International Journal of Theoretical Physics **46**, 1786 (2007).
[41] A.R. Plastino, A. Puente, M. Casas, F. Garcias and A. Plastino, Revista Mexicana de Física **46**, 78 (2000).
[42] O. Mustafa, Phys. Lett. A **384**, 126265 (2020).
[43] A.R. Plastino, A. Rigo, M. Casas, F. Garcias and A. Plastino, Phys. Rev. A **60**, 4318 (1999).
[44] J. Guo-Xing, C. Chang-Ying and R. Zhong-Zhou, Communications in Theoretical Physics **51**, 797 (2009).
[45] J.P.G. Nascimento and I. Guedes, Revista Brasileira de Ensino de Física **38**, e2315 (2016).
[46] D.J. Griffiths and D.F. Schroeter, *Introduction to Quantum Mechanics* (Cambridge University Press, Cambridge, 2018), 3 ed.